Journal of Alloys and Compounds 776 (2019) 149–155

Contents lists available at ScienceDirect

Journal of Alloys and Compounds

journal homepage: http://www.elsevier.com/locate/jalcom

Enhanced photoelectric response of plasmon-active ZnO nanorods by spatial modulation of dielectric environment

Guohua Liu [a, b], Phuong Dao [b], Vy Nguyen [b], Kang Du [b], Chaoqun Cheng [b], Jinliang Xu [a], Kaiying Wang [b, *]

[a] Beijing Key Laboratory of Multiphase Flow and Heat Transfer for Low Grade Energy Utilization, North China Electric Power University, Beijing, 102206, PR China

[b] Department of Micro and Nano Systems Technology, University of South-Eastern Norway, Horten, 3184, Norway

ARTICLE INFO

Article history:
Received 31 July 2018
Received in revised form
16 October 2018
Accepted 19 October 2018
Available online 21 October 2018

Keywords:
ZnO nanorods
Surface plasmon resonant
Dielectric layer
Photoresponse

ABSTRACT

One-dimensional zinc oxide (ZnO) nanorods have excellent electron mobility and exhibit great potential for photoelectric or photochemical applications. However, poor visible light absorption and rapid surface charge recombination are bottleneck for promoting its applications. In this work, plasmonic gold nanoparticles (Au NPs) and dielectric silicon oxide (SiO_2) are deposited on the surface of ZnO nanorods to tune their photoelectric performance. The localized surface plasmon resonance of Au NPs extends the absorption spectrum to visible region. The surface passivation with dielectric SiO_2 layer suppresses the photoexcited electron-hole recombination. By rational integration of the configuration, it is found that dielectric spacer (ZnO-SiO_2-Au) shows obvious photocurrent improvement. While dielectric shell-coating (ZnO-Au-SiO_2) dramatically leads to an outstanding photocurrent enhancement, which is ~4 −28 times higher than that of the other counterparts. The enhanced performance is ascribed to its effectiveness for spatially separating electron-hole pairs and optimizing photo-absorption properties of the metal-semiconductor system. This strategy provides new insights into fabrication of high performance light harvesting antenna, and stands for a basis to design solar-active systems.

1. Introduction

Metal oxides such as titanium dioxide, zinc oxide and hematite oxide have shown great potential as photoelectrodes in photoelectric or photoelectrochemical cells [1–3]. Among them, ZnO presents a unique crystalline structure, a direct wide band gap (3.37 eV), a large exciton binding energy, excellent electron mobility and environmental compatibility [4–6]. One-dimensional ZnO nanorods attract more attention owning to their high aspect ratio, large specific surface area, high photon-induced charges generation and transfer rate [4,7–11]. However, the large bandgap restricting its utilization in visible light range of solar spectrum and the high recombination rate of photogenerated electrons and holes leading to a low quantum yield and poor photoelectric properties. Various methods have been proposed for improving the photoelectric conversion efficiency across the entire ultraviolet–visible spectrum, such as doping or introducing defects, crystal growth control, surface modification, and the creation of heterostructures, etc [12,13].

The decoration of semiconductor with metal nanoparticles (NPs) is one promising ways to improve the photoelectric conversion efficiency. This is because metal NPs have the unique ability to concentrate light through plasmonic enhancement of the local field and thereby enhance the light-matter interactions in adjacent materials [2,14,15]. The remarkable features of plasmon-induced photophysics is surface plasmon resonance (SPR), which arises from the collective oscillation of free electrons at the metallic interface or in small metallic nanostructures. The plasmon metal-semiconductor structures confer several distinct advantages [16,17]. First, plasmonic metal nanoparticles act as photosensitizers in metal-semiconductor junctions and strongly absorb at specific wavelengths in the visible region. Second, the metallic nanoparticles effectively act as antenna, which are useful in semiconductors with a short minority carrier diffusion length. Therefore, under visible light irradiation, the continuously injected hot-electrons from metal nanostructure into conduction band of semiconductor as well as formation of Schottky barrier facilitates

* Corresponding author.
E-mail address: Kaiying.Wang@usn.no (K. Wang).

https://doi.org/10.1016/j.jallcom.2018.10.233
0925-8388/

electron-hole separation and promotes the photoelectrical performance [18].

Although tuning SPR by size, shape and distribution of noble metal has been widely explored, the surrounding environments are key parameter from physics point of view [18–21]. It was found that the plasmon resonant frequency and intensity intimately related to the dielectric properties of surrounding environment [14,22–24]. Besides, the semiconductor suffers electrolyte corrosion during the photoelectrochemical process, the presence of gold metal nanoparticles and dielectric oxide layer such as silicon dioxide could improve the photochemical stability [2,3,25]. Moreover, SiO_2 coating as dielectric circumstance enables higher refractive index resulting in a red shift and stronger localization of electromagnetic field [23,26,27]. Therefore, rational integration of functional components in composite nanostructures is important for solar energy harvesting since that is advantageous to extend the light absorption, reduces the charge carrier recombination and resists the electrolyte corrosion simultaneously.

In this work, we investigate the light harvesting and photoelectrochemical performance of ternary heterojunctions by introducing Au NPs and SiO_2 overlayer on ZnO nanorods. The ZnO nanorods is synthesized on ITO glass by a two-step fabrication process. Au NPs and SiO_2 film are sputtered on the nanorods with diverse spatial configurations. The optimal size of Au particle and the thickness of SiO_2 overlayer are acquired through precise controlling the duration of sputtering. The results show that the dielectric shell-coating nanorods ZnO-Au-SiO_2 deliver the best photocurrent density response compared to the other references. Such enhancement is ascribed to the synergistic effect of SPR induced by Au NPs and surface passivation resulted from the dielectric SiO_2 overlayer.

2. Experimental

2.1. Material preparation

The raw material zinc nitrate [$Zn(NO_3)_3$], absolute ethanol, zinc acetate [$Zn(CH_3CO_2)_2$], hexamethylenetetramine and indium tin oxide (ITO) coated glasses were purchased from Sigma-Aldrich. All chemicals were used as received without further treatment. Nanorods ZnO were synthesized on ITO glass via a two-step process. To prepare the seeding solution, 10 ml of zinc acetate 0.08 M in absolute ethanol with addition of 0.25 ml water were stirred for 2 h. The ITO substrate was dipped into zinc acetate solution for 20 s with a fixed withdrawing speed and then dried in oven at 75 °C for 35 min. This process was repeated four times. The seeded substrate was then annealed in air at 220 °C for 1 h and immersed up side down in the solution of 0.025 M zinc nitrate and hexamethylenetetramine. The hydrothermal treatment was conducted at 90 °C in 4 h. Finally, the ITO glass was rinsed several times with water and ethanol, dried at room temperature and calcined at 450 °C in 30 min.

During the sputtering process, Au and SiO_2 films were prepared by radio frequency magnetron sputtering. A cleaned FTO substrate and the sample were placed parallel to the target at room temperature. For the reference, a thin layer of film were deposited onto the FTO substrate and annealed under the same annealing conditions for estimating the deposition thickness [28]. The Au sputter coater (VG Microtech SC500) was operated at 10 mA for 110 s with the vacuum pressure of Argon process level at 10^{-2} mbar to produce approximately 5 nm of the film. By controlling the sputtering duration and the annealing process, the film thickness could be can be flexible tuned in the range of 5–20 nm. The tools SEM and TEM have been used to characterize the film thickness and particle size. For the thin film SiO_2 sputtering process (5 nm, AJA sputter), the Ar flow at 5 sccm, the power applied to the SiO_2 target is 130 W and the pressure is 3.3 mTorr. By the sputtering process with various loading orders. Five spatial configurations including ZnO, ZnO-SiO_2, ZnO-Au, ZnO-SiO_2-Au, ZnO-Au-SiO_2 were fabricated by using magnetron sputtering on ZnO nanorod arrays (Fig. 1).

2.2. Characterization

Surface morphology and detailed microscopic structure of the samples were analyzed using scanning electron microscope (SEM, Hitachi 1081) at 30 kV accelerating voltage and transmission electron microscope (TEM, JEOL JEM2100F). The high angle annular dark field (HAADF) and energy-dispersive X-ray spectroscopy (EDS) were acquired on a FEI TalosF200X. The light absorption spectra were recorded on a spectrophotometer (SHIMADZU, UV-2600 with ISR-2600 integrating sphere attachment) in range of 220–850 nm with fine $BaSO_4$ powder as reference. The electrochemical characterization was conducted using three electrode methods with a standard electrochemical workstation (Zahner elektrik IM6). The ITO glass with difference loadings on nanorods ZnO (effective layer 1 cm^2) was used as the working electrode following by Ag/AgCl and Pt electrode as the reference and counter electrode, respectively. The solution 0.5 M Na_2SO_4 (pH = 6.8) was the supporting electrolyte for all measurement. A light source (halogen lamp 15 V/150 W) is utilized to record the photocurrent in visible region with bias of +0.3, +0.5 and + 0.7 V.

3. Results and discussion

3.1. Morphology and structure

Fig. 2a shows a photograph of the samples including ZnO, ZnO-SiO_2, ZnO-Au, ZnO-SiO_2-Au, ZnO-Au-SiO_2 nanorod arrays. It can be seen that first two samples of ZnO, ZnO-SiO_2 exhibit semi-transparent color, while the color of other samples change to dark grey after introducing gold nanoparticles, suggesting that they absorb a considerable portion of visible light. Fig. 2b and c shows a series of scanning electron microscopy (SEM) images of the nanorod composites ZnO-Au-SiO_2, which has uniform size and ordered shape with a diameter about 300–350 nm and length of 1–2 μm. The high-resolution image (Fig. 2c) indicates that small nanoparticles distributed on the surface of nanorods.

The transmission electron microscopy images (Fig. 3a and b) provide a more distinct comparison and confirmation for the nanorod ZnO-Au-SiO_2. It is clearly seen that the sample is an assembly of uniform three dimensionally ordered core-shell nanoparticles on the nanorod. The high-resolution image (Fig. 3a) shows the lattice fringes of crystalline component. The back scattered electron image in Fig. 3b shows the nanoparticles are evenly distributed on the nanorod surface and the average size of particle is around 8 nm (~10% errors). Compared with small Au NPs, the Au-SiO_2 core-shell NPs are not easier to aggregate as the surface energy is relatively lower. The selected SAED pattern (Fig. 3c) reveals the crystalline nature of nanorods as the spotted rings and dots can be detected.

The element distribution maps of the nanorod are shown in Fig. 3d. HAADF and elemental maps confirm the co-existence of Au, Si and O, that they are homogeneously dispersed on the surface of ZnO nanorod. The mapping image of Si shows Au NPs are capped with SiO_2, which further confirms the formation of core-shell structure (Fig. 3a). The interface between the ZnO and Au core is expected to be important for the hot-electron injection from Au to the conductive band (CB) of ZnO upon localized surface plasmon resonant (LSPR) excitation. A single nanorod is further analyzed using EDS spectrum to detect distribution of individual elements

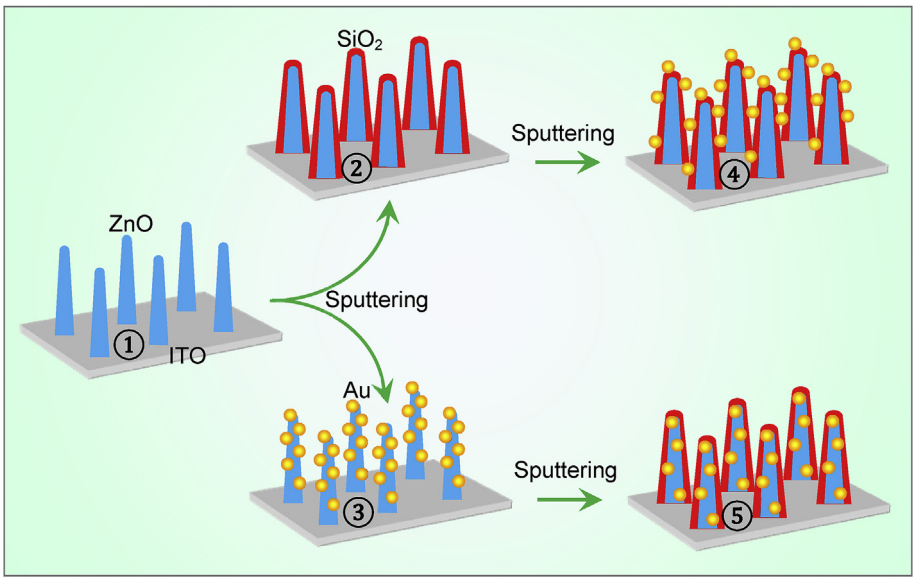

Fig. 1. Schematic illustration of fabrication process of the nanorod arrays.

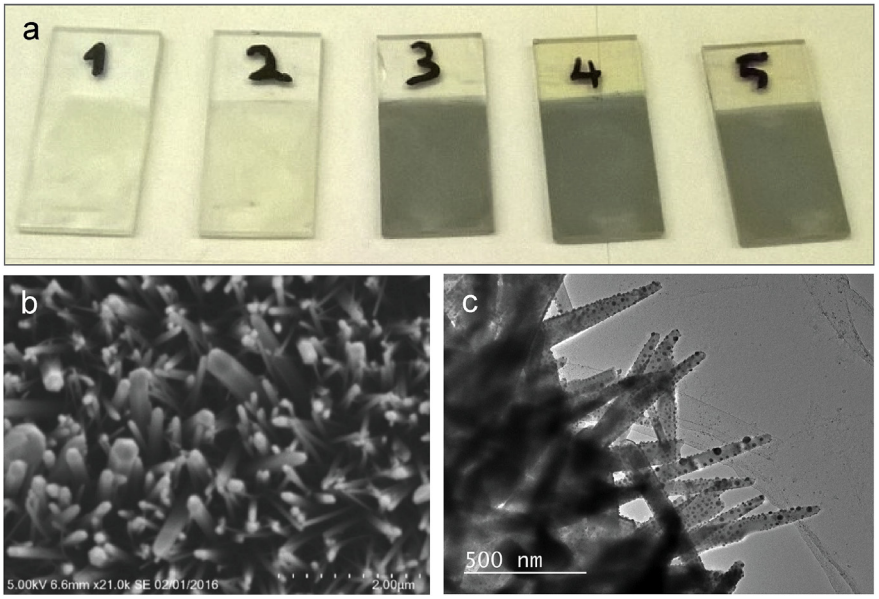

Fig. 2. a) A photograph of the resulting samples of ZnO, ZnO-SiO_2, ZnO-Au, ZnO-SiO_2-Au, ZnO-Au-SiO_2, corresponding to the samples in Fig. 1b) and c) SEM images of ZnO nanorods with Au and SiO_2 deposition.

(Fig. 3e). The Au, Si, Zn and O peaks along with Cu and C peaks can be clearly observed in the spectrum, demonstrating their co-existence in the composite. The ratio between Zn and O is roughly unity presenting for ZnO with small amount of gold (8.46%.at) that uniformly dispersed on the surface of nanorod. Due to the nature and thin layer of silicon oxide (<5 nm), it is hard to be detected in the EDS spectrum.

3.2. Light absorption and photoelectric properties

Fig. 4a shows the UV–vis absorption spectra of ZnO nanorods, ZnO-SiO_2 and ZnO-Au nanorods (two components), ZnO-SiO_2-Au and ZnO-Au-SiO_2 nanorods (three components), respectively. All the samples are of the same size and thickness. For ZnO nanorods, the strong absorption at wavelength range below 400 nm matches the intrinsic interband transition absorption of ZnO, exhibiting its UV absorption properties. The nanorods with thin film SiO_2 on ZnO performs stronger light absorption than pristine ZnO, which could be explained by the higher refractive index properties of SiO_2. In this manner, the charge-carrier generation, separation and collection of ZnO can be improved by means of resonant light trapping in ultrathin SiO_2 films designed as optical cavities. Interference between forward- and backward-propagating waves enhances the light absorption in quarter-wave, amplifying the intensity close to the surface wherein photogenerated minority charge carriers can reach the surface [29,30]. While the gold decorated nanorods show a broad peak at 600 nm, corresponding to SPR absorption of Au nanoparticles, which could be tuned by varying their size, shape and surrounding environment [14,20]. After the deposition of SiO_2 on Au nanoparticles, the SPR absorption peak red-shifts to 620 nm

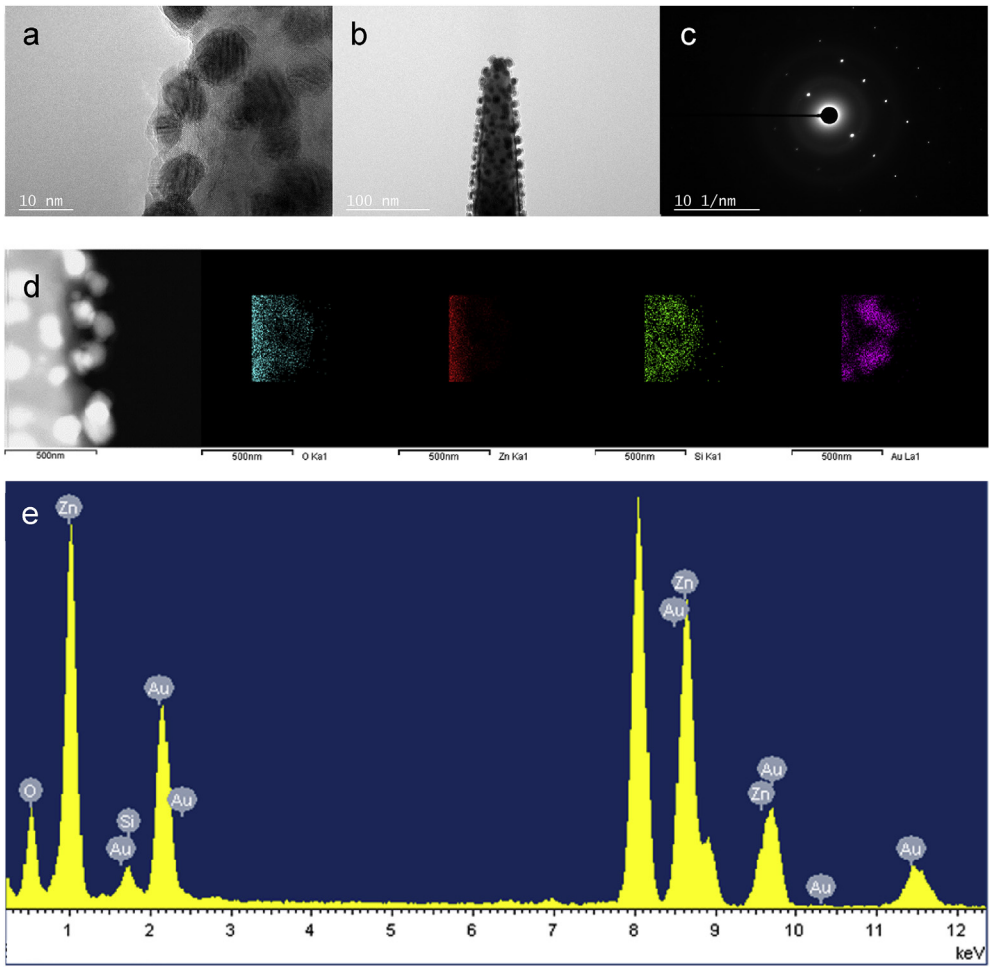

Fig. 3. a) and b) TEM images of a ZnO nanorod with Au and SiO_2 deposition. c) Selected Area Electron Diffraction (SAED) images of the sample. d) The high angle annular dark field (HAADF) and Energy-dispersive X-ray spectroscopy (EDS) elemental mapping image of the sample. e) EDS spectrum.

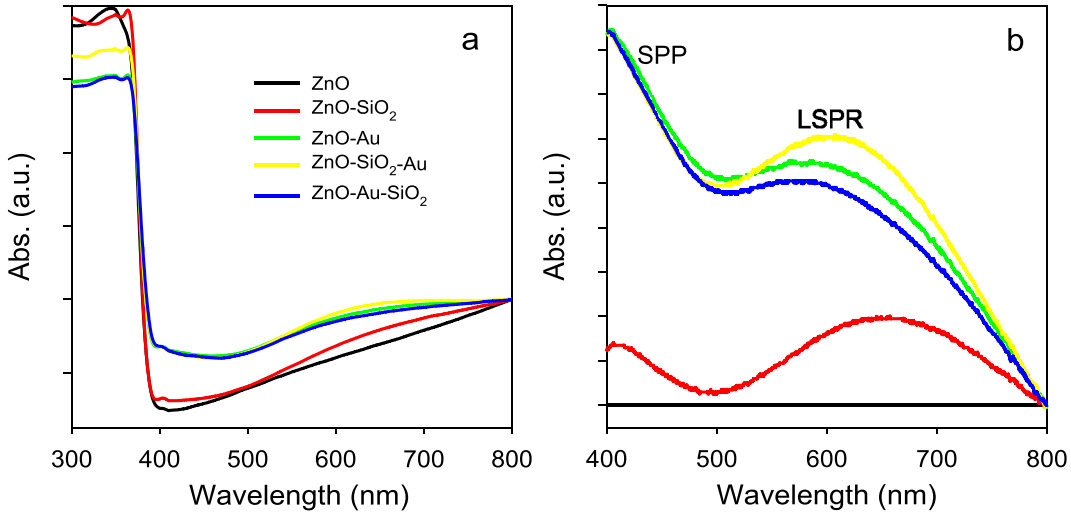

Fig. 4. a) UV–vis absorption spectra of the nanorods with and without coating, b) the absorption spectra by substracting the spectra of ZnO.

because of the strong electromagnetic coupling of Au and SiO_2. This implies that the SiO_2 with higher dielectric constant directly contacting with Au NPs would lead to red shift of the SPR band [14].

The SPR exists in two distinct forms: surface plasmon polaritons (SPP) and LSPR [31]. SPP or propagating surface plasmons are travelling charge oscillations resonantly excited on the surface of thin metal films, whereas LSPR is the stationary, non-propagating collective oscillation of the surface electrons in metal

nanostructures. SPP and LSPR in plasmonic nanostructures improve the solar energy conversion efficiency of semiconductors via two pathways: photonic enhancement and plasmonic energy-transfer enhancement. In present work, the nanorods act as miniature fiber optics to create the confined modes, which traps the incident light to enhance the light absorption [32,33]. The intense local field enhancement of the LSPR overlapped with the absorption band edge of ZnO, enhancing solar energy harvesting at the energies below the band edge through the resonance energy transfer mechanism [34]. As a result, the photonic (~425 nm) and the plasmonic energy-transfer enhancement (~650 nm) are observed in the absorption spectrum (Fig. 4b).

Fig. 5a displays linear sweep voltammogram curves of the samples versus Ag/AgCl applied potential from 0.0 to 0.8 V under visible-light illumination. For the ZnO and ZnO-SiO_2 nanorods, their photocurrents are relatively low. The ZnO-Au-SiO_2 nanorods present the highest photocurrent, while ZnO-SiO_2-Au exhibits a lower value as compared to gold decorated ZnO. Fig. 5b shows photoresponse of the samples at 0.5 V vs. Ag/AgCl under light illumination. It can be seen that the bare ZnO or ZnO-SiO_2 nanorod

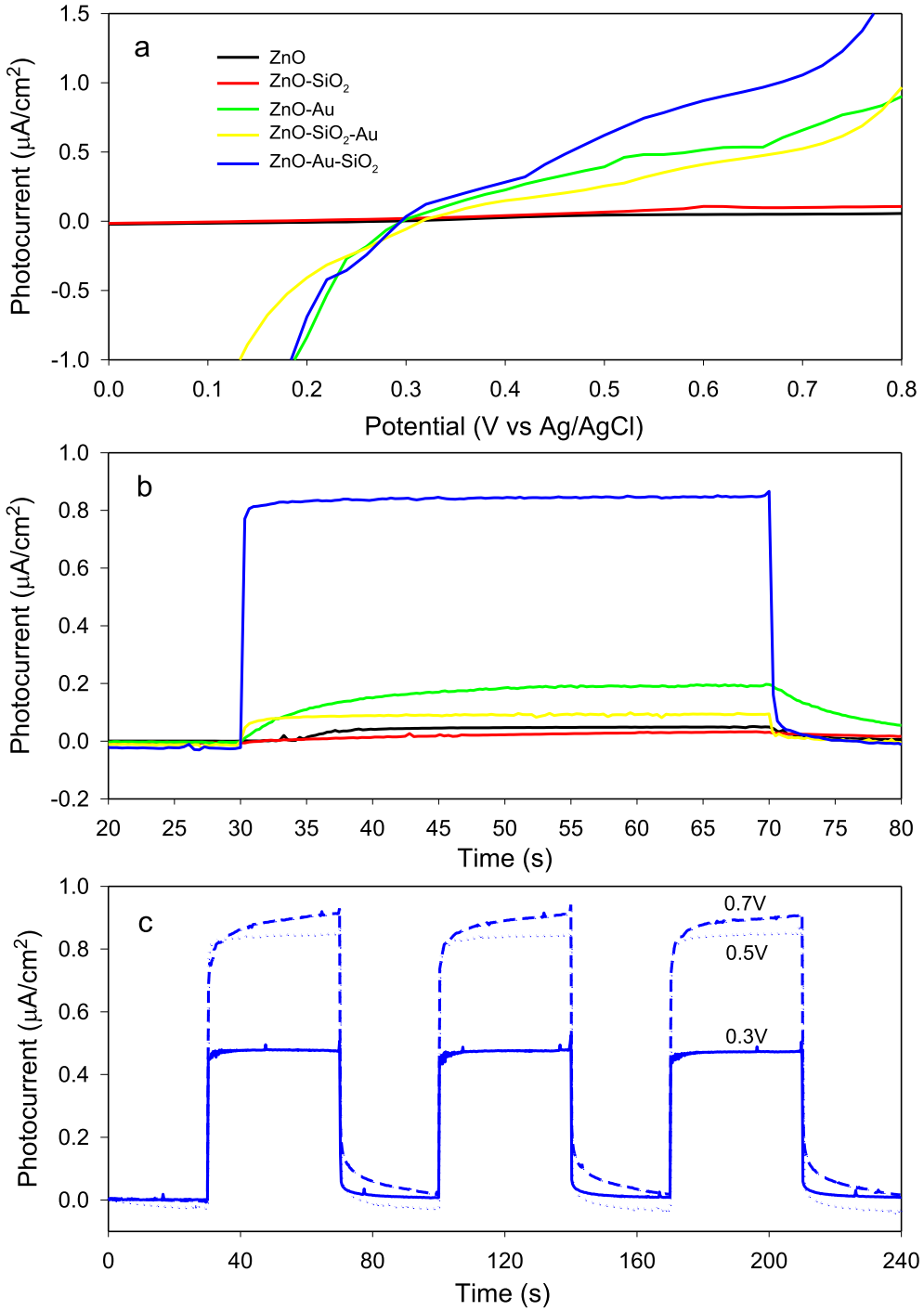

Fig. 5. a) I-V curves of the nanorods ZnO, Zn-SiO_2, Zn-Au, ZnO-SiO_2-Au, ZnO-Au-SiO_2 under white light illumination b) Photoresponses of the nanorods at 0.5 V bias under white light illumination c) Transient photoresponse of the nanorods ZnO-Au-SiO_2 at 0.3, 0.5, 0.7 V bias.

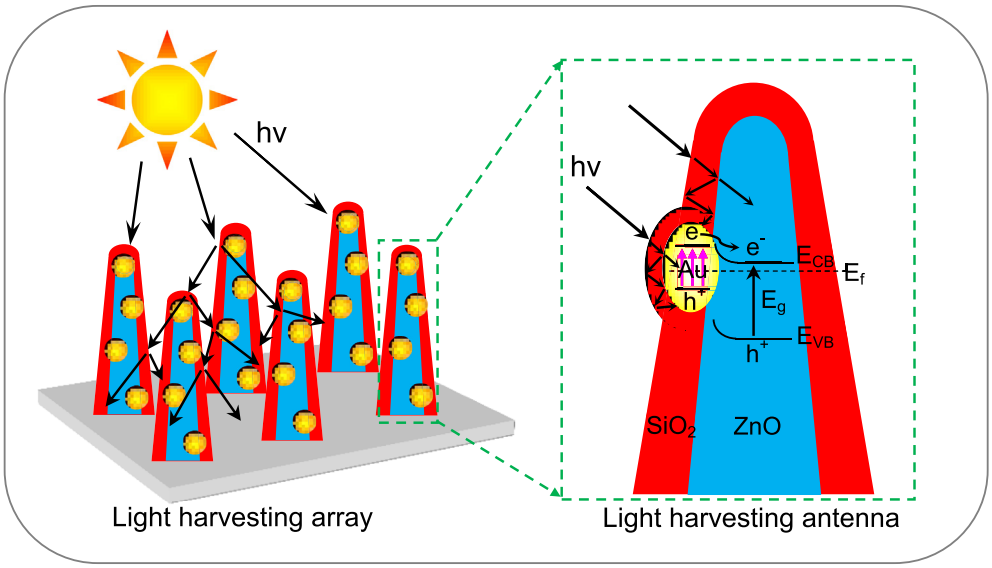

Fig. 6. Light harvesting mechanisms and photoelectrical physics.

array almost does not produce photocurrent. Most of the responses present in a pulse shape corresponding to light excitation. The ZnO-Au-SiO_2 nanorods show the fastest photoresponse once the light is turned on, and exhibit a maximum current density of 0.86 μA/cm^2, which is about 4.3, 9.6, 17.2 and 28.7 times compared with the values of ZnO-Au (0.20 μA/cm^2), ZnO-SiO_2-Au (0.09 μA/cm^2), ZnO (0.05 μA/cm^2) and ZnO-SiO_2 (0.03 μA/cm^2). Fig. 5c shows the transient photoresponse of ZnO-Au-SiO_2 nanorods, which exhibits a good reproducible photocurrent density over the times at different bias. This clearly confirms that the nanorod arrays have superior visible-light photoelectrochemical properties.

3.3. *Light harvesting mechanism and photoelectrical physics*

Due to chemical inertness and light transparency, SiO_2 has been utilized as a stabilizer, protecting, passive or dielectric layer in a series of photoelectric and photochemical applications. As a protecting layer, SiO_2 retards the interaction with oxygen and results in electron-hole recombination [3,25]. This recombination significantly reduces the photocurrent (Fig. 5b). While gold nanoparticles loaded ZnO nanorods is a well-known plasmonic structure under visible light irradiation [5,35]. Therefore, gold nanoparticles loaded ZnO nanorods shows strong visible light absorption due to the plasmonic effect. Besides, the incorporating gold with ZnO results in the Schottky barrier at the contact interface causing the band bending. The hot electrons with enough energetic potential jump through the Schottky barrier into the CB of ZnO (Fig. 6). In ZnO-SiO_2-Au configuration, the dielectric SiO_2 layer acts as insulator between gold nanoparticles and ZnO nanorods. This dielectric layer weakens the electromagnetic field intensity, which depresses the electron-hole separation. On the other hand, under visible light irradiation, the energetic electron can tunnel through the thin film SiO_2 to inject into the nanorods ZnO [36]. Therefore, the photocurrent of ZnO-SiO_2-Au is lower than the gold decorated ZnO nanorods but still higher than that of the pristine ZnO nanorods.

Interestingly, ZnO-Au-SiO_2 nanorods exhibit an outstanding photoresponse. There are several reasons contributing for this high photocurrent density. Firstly, gold plasmonic structures have the possibility to interact with the electrolyte components that decreases the amount of energetic electrons injected into the ZnO nanorods. The thin layer SiO_2 inhibits the electron in conduction state interacting with the electrolyte, which not only increases the electron injection efficiency from photoexcited Au nanoparticles, but also suppresses the possibility of charge recombination [37]. Secondly, the structure exhibits more intensive electromagnetic field at the semiconductor-plasmonic metal interface as well as deeper penetration into the semiconductor than the other counterparts. This greatly increases the light absorption cross-section of plasmonic nanoparticle [38–40]. In addition, as compared to electrolyte, the higher refractive index of dielectric layer and multi-scattering effect induced by nanorods establish light-trapping structures, which extends the pathway of incident light [30,41–43]. Therefore, the light-trapping structures enhance the light absorption of the sample, reflecting in an enhanced photocurrent.

4. Conclusions

In this work, Au NPs and SiO_2 overlayer are synergistically integrated on ZnO nanorods for solar energy harvesting. Photoelectric behavior of the gold and silicon oxide decorated ZnO nanorods are explored under solar irradiation. As a result, the increased absorption in visible region due to the SPR effect and the enhanced photogenerated electron-hole separation originated from the surface passivation lead to a significantly improved photoelectric performance. The ZnO-Au-SiO_2 nanorods exhibit superior photoresponse that is ~4 times higher than that of the ZnO-Au nanorods. This is ascribed to 1) the dielectric SiO_2 intensifies SPR-mediated hot electron injection, 2) the effective electron transfer channel through the ZnO backbone, 3) the light trapping structures due to its higher dielectric index and multi-scattering effect induced by photonic nanorod arrays. While the presence of thin dielectric layer between gold and ZnO nanorods weakens the response to visible light owning to the electromagnetic inhibition induced by passivation effect. The rational design of plasmonic-dielectric-semiconductor system paves a new avenue to develop highly efficient photoactive materials for solar energy harvesting.

Notes

The authors declare no competing financial interest.

Acknowledgements

Research was supported with grants from the Nature Science Foundation of China (51576002) and the Norwegian Research Council-Independent Projects-Mathematics, Physical Science and Technology Programme (FRINATEK-231416/F20).

References

[1] X. Liu, J. Iocozzia, Y. Wang, X. Cui, Y. Chen, S. Zhao, Z. Li, Z. Lin, Noble metal-metal oxide nanohybrids with tailored nanostructures for efficient solar energy conversion, photocatalysis and environmental remediation, Energy Environ. Sci. 10 (2017) 402–434.
[2] W.R. Erwin, H.F. Zarick, E.M. Talbert, R. Bardhan, Light trapping in mesoporous solar cells with plasmonic nanostructures, Energy Environ. Sci. 9 (2016) 1577–1601.
[3] G. Liu, K. Du, J. Xu, G. Chen, M. Gu, C. Yang, K. Wang, H. Jakobsen, Plasmon-dominated photoelectrodes for solar water splitting, J. Mater. Chem. A 5 (2017) 4233–4253.
[4] Y. Liu, X. Yan, Z. Kang, Y. Li, Y. Shen, Y. Sun, L. Wang, Y. Zhang, Synergistic effect of surface plasmonic particles and surface passivation layer on ZnO nanorods array for improved photoelectrochemical water splitting, Sci. Rep. 6 (2016) 29907.
[5] C. Li, X. Zhu, H. Zhang, Z. Zhu, B. Liu, C. Cheng, 3D ZnO/Au/CdS sandwich structured inverse opal as photoelectrochemical anode with improved performance, Adv. Mater. Interfaces 2 (2015), 1500428.
[6] C. Li, Z. Zang, C. Han, Z. Hu, X. Tang, J. Du, Y. Leng, K. Sun, Highly compact $CsPbBr_3$ perovskite thin films decorated by ZnO nanoparticles for enhanced random lasing, Nano Energy 40 (2017) 195–202.
[7] M. Prasad, V. Sharma, R. Aher, A. Rokade, P. Ilaiyaraja, C. Sudakar, S. Jadkar, Synergistic effect of Ag plasmon- and reduced graphene oxide-embedded ZnO nanorod-based photoanodes for enhanced photoelectrochemical activity, J. Mater. Sci. 52 (2017) 13572–13585.
[8] V.R. Kopach, K.S. Klepikova, N.P. Klochko, I.I. Tyukhov, G.S. Khrypunov, V.E. Korsun, V.M. Lyubov, A.V. Kopach, R.V. Zaitsev, M.V. Kirichenko, Solar active Ag/ZnO nanostructured arrays obtained by a combination of electrochemical and chemical methods, Sol. Energy 136 (2016) 23–31.
[9] W. Zhang, W. Wang, H. Shi, Y. Liang, J. Fu, M. Zhu, Surface plasmon-driven photoelectrochemical water splitting of aligned ZnO nanorod arrays decorated with loading-controllable Au nanoparticles, Sol. Energy Mater. Sol. Cells 180 (2018) 25–33.
[10] S. Ren, Y. Wang, G. Fan, R. Gao, W. Liu, Sandwiched ZnO@Au@CdS nanorod arrays with enhanced visible-light-driven photocatalytical performance, Nanotechnology 28 (2017), 465403.
[11] N. Patra, S.K. Karuturi, N.J. Vasa, D. Nakamura, M. Higashihata, V. Singh, I.A. Palani, Influence of Ni, Ti and NiTi alloy nanoparticles on hydrothermally grown ZnO nanowires for photoluminescence enhancement, J. Alloys Compd. 770 (2019) 1119–1129.
[12] Ü. Özgür, Y.I. Alivov, C. Liu, A. Teke, M.A. Reshchikov, S. Doğan, V. Avrutin, S.J. Cho, H. Morkoç, A comprehensive review of ZnO materials and devices, J. Appl. Phys. 98 (2005), 041301.
[13] V.P. Dinesh, A. Sukhananazerin, P. Biji, An emphatic study on role of spill-over sensitization and surface defects on NO_2 gas sensor properties of ultralong ZnO@Au heterojunction NRs, J. Alloys Compd. 712 (2017) 811–821.
[14] N. Jiang, X. Zhuo, J. Wang, Active plasmonics: principles, structures, and applications, Chem. Rev. 118 (2018) 3054–3099.
[15] J.B. Lee, S. Choi, J. Kim, Y.S. Nam, Plasmonically-assisted nanoarchitectures for solar water splitting: obstacles and breakthroughs, Nano Today 16 (2017) 61–81.
[16] S. Yu, Y.H. Kim, S.Y. Lee, H.D. Song, J. Yi, Hot-electron-transfer enhancement for the efficient energy conversion of visible light, Angew. Chem. 53 (2014) 11203–11207.
[17] G. Liu, H. Cao, J. Xu, Solar evaporation of a hanging plasmonic droplet, Sol. Energy 170 (2018) 184–191.
[18] S.H. Lee, S.W. Lee, T. Oh, S.H. Petrosko, C.A. Mirkin, J.W. Jang, Direct observation of plasmon-induced interfacial charge separation in metal/semiconductor hybrid nanostructures by measuring surface potentials, Nano Lett. 18 (2018) 109–116.
[19] A. Gołąbiewska, A. Malankowska, M. Jarek, W. Lisowski, G. Nowaczyk, S. Jurga, A. Zaleska-Medynska, The effect of gold shape and size on the properties and visible light-induced photoactivity of Au-TiO_2, Appl. Catal., B 196 (2016) 27–40.
[20] K.L. Kelly, E. Coronado, L.L. Zhao, G.C. Schatz, The optical properties of metal nanoparticles: the influence of size, shape, and dielectric environment, J. Phys. Chem. B 107 (2003) 668–677.
[21] N. Zhang, C. Han, Y.-J. Xu, J.J. Foley Iv, D. Zhang, J. Codrington, S.K. Gray, Y. Sun, Near-field dielectric scattering promotes optical absorption by platinum nanoparticles, Nat. Photon. 10 (2016) 473–482.
[22] T. Butburee, Y. Bai, J. Pan, X. Zong, C. Sun, G. Liu, L. Wang, Step-wise controlled growth of metal@TiO_2 core-shells with plasmonic hot spots and their photocatalytic properties, J. Mater. Chem. A 2 (2014) 12776.
[23] S.K. Medda, S. De, G. De, Synthesis of Au nanoparticle doped SiO_2-TiO_2 films: tuning of Au surface plasmon band position through controlling the refractive index, J. Mater. Chem. 15 (2005) 3278.
[24] Z. Yue, B. Cai, L. Wang, X. Wang, M. Gu, Intrinsically core-shell plasmonic dielectric nanostructures with ultrahigh refractive index, Sci. Adv. 2 (2016), e1501536.
[25] P. Mulvaney, L.M. Liz-Marzán, M. Giersig, T. Ung, Silica encapsulation of quantum dots and metal clusters, J. Mater. Chem. 10 (2000) 1259–1270.
[26] J.F. Li, Y.F. Huang, Y. Ding, Z.L. Yang, S.B. Li, X.S. Zhou, F.R. Fan, W. Zhang, Z.Y. Zhou, D.Y. Wu, B. Ren, Z.L. Wang, Z.Q. Tian, Shell-isolated nanoparticle-enhanced Raman spectroscopy, Nature 464 (2010) 392–395.
[27] F.F. Abdi, A. Dabirian, B. Dam, R. van de Krol, Plasmonic enhancement of the optical absorption and catalytic efficiency of $BiVO_4$ photoanodes decorated with Ag@SiO_2 core-shell nanoparticles, Phys. Chem. Chem. Phys. 16 (2014) 15272–15277.
[28] W. Chen, Y. Lu, W. Dong, Z. Chen, M. Shen, Plasmon mediated visible light photocurrent and photoelectrochemical hydrogen generation using Au nanoparticles/TiO_2 electrode, Mater. Res. Bull. 50 (2014) 31–35.
[29] H. Dotan, O. Kfir, E. Sharlin, O. Blank, M. Gross, I. Dumchin, G. Ankonina, A. Rothschild, Resonant light trapping in ultrathin films for water splitting, Nat. Mater. 12 (2013) 158–164.
[30] M.A. Kats, R. Blanchard, P. Genevet, F. Capasso, Nanometre optical coatings based on strong interference effects in highly absorbing media, Nat. Mater. 12 (2013) 20–24.
[31] J. Li, S.K. Cushing, P. Zheng, F. Meng, D. Chu, N. Wu, Plasmon-induced photonic and energy-transfer enhancement of solar water splitting by a hematite nanorod array, Nat. Commun. 4 (2013) 2651.
[32] L. Cao, P. Fan, A.P. Vasudev, J.S. White, Z. Yu, W. Cai, J.A. Schuller, S. Fan, M.L. Brongersma, Semiconductor nanowire optical antenna solar absorbers, Nano Lett. 10 (2010) 439–445.
[33] M. Anaya, M.E. Calvo, J.M. Luque-Raigon, H. Miguez, Resonant photocurrent generation in dye-sensitized periodically nanostructured photoconductors by optical field confinement effects, J. Am. Chem. Soc. 135 (2013) 7803–7806.
[34] J. Li, S.K. Cushing, F. Meng, T.R. Senty, A.D. Bristow, N. Wu, Plasmon-induced resonance energy transfer for solar energy conversion, Nat. Photon. 9 (2015) 601–607.
[35] Q. Liu, Y. Wei, M.Z. Shahid, M. Yao, B. Xu, G. Liu, K. Jiang, C. Li, Spectrum-enhanced Au@ZnO plasmonic nanoparticles for boosting dye-sensitized solar cell performance, J. Power Sources 380 (2018) 142–148.
[36] L. Chen, J. Yang, S. Klaus, L.J. Lee, R. Woods-Robinson, J. Ma, Y. Lum, J.K. Cooper, F.M. Toma, L.W. Wang, I.D. Sharp, A.T. Bell, J.W. Ager, p-Type transparent conducting oxide/n-type semiconductor heterojunctions for efficient and stable solar water oxidation, J. Am. Chem. Soc. 137 (2015) 9595–9603.
[37] I. Thomann, B.A. Pinaud, Z. Chen, B.M. Clemens, T.F. Jaramillo, M.L. Brongersma, Plasmon enhanced solar-to-fuel energy conversion, Nano Lett. 11 (2011) 3440–3446.
[38] K. Awazu, M. Fujimaki, C. Rockstuhl, J. Tominaga, H. Murakami, Y. Ohki, N. Yoshida, T. Watanabe, A plasmonic photocatalyst consisting of silver nanoparticles embedded in titanium dioxide, J. Am. Chem. Soc. 130 (2008) 1676–1680.
[39] Z.W. Seh, S. Liu, M. Low, S.Y. Zhang, Z. Liu, A. Mlayah, M.Y. Han, Janus Au-TiO_2 photocatalysts with strong localization of plasmonic near-fields for efficient visible-light hydrogen generation, Adv. Mater. 24 (2012) 2310–2314.
[40] M. Li, M. Li, Y. Zhu, Y. Tang, L. Bai, W. Lei, Z. Wang, X. Zhao, Scattering and plasmonic synergetic enhancement of the performance of dye-sensitized solar cells by double-shell SiO_2@Au@TiO_2 microspheres, Nanotechnology 28 (2017), 265202.
[41] X. Zheng, L. Zhang, Photonic nanostructures for solar energy conversion, Energy Environ. Sci. 9 (2016) 2511–2532.
[42] Z. Zhang, L. Zhang, M.N. Hedhili, H. Zhang, P. Wang, Plasmonic gold nanocrystals coupled with photonic crystal seamlessly on TiO_2 nanotube photoelectrodes for efficient visible light photoelectrochemical water splitting, Nano Lett. 13 (2013) 14–20.
[43] X. Zhang, Y. Liu, S.-T. Lee, S. Yang, Z. Kang, Coupling surface plasmon resonance of gold nanoparticles with slow-photon-effect of TiO_2 photonic crystals for synergistically enhanced photoelectrochemical water splitting, Energy Environ. Sci. 7 (2014) 1409.